NASA Technical Memorandum 81377

ACOUSTIC CONSIDERATIONS OF FLIGHT EFFECTS ON JET NOISE SUPPRESSOR NOZZLES

U. von Glahn
Lewis Research Center
Cleveland, Ohio

Prepared for the
Eighteenth Aerospace Sciences Meeting
sponsored by the American Institute of Aeronautics and Astronautics
Pasadena, California, January 14-16, 1980

AIAA Paper No. 80-0164

ACOUSTIC CONSIDERATIONS OF FLIGHT EFFECTS ON JET NOISE SUPPRESSOR NOZZLES

U. von Glahn

National Aeronautics and Space Administration
Lewis Research Center
Cleveland, Ohio 44135

Abstract

Insight into the inflight acoustic characteristics of high-velocity jet noise suppressor nozzles for supersonic cruise aircraft (SCA) is provided. Although the suppression of jet noise over the entire range of directivity angles is of interest, the suppression of the peak noise level in the rear quadrant is frequently of the most interest. Consequently, the paper is directed primarily to the inflight effects at the peak noise level. Both single and inverted-velocity-profile multistream suppressor nozzles are considered. The importance of static spectral shape on the noise reduction due to inflight effects is stressed.

Introduction

In order for supersonic cruise aircraft to meet at least the FAR-36 (1969) noise rule, the use of variable cycle engines (VCE) utilizing coannular inverted-velocity-profile nozzles or low bypass (two stream) engines with suppressor nozzles have been advocated in recent years. With the introduction of the FAR-36 (1977) noise goals, and even more stringent noise goals proposed for the future, all practical current engine cycles being considered will require jet noise suppressor nozzles.

In order to assess the impact of supersonic cruise aircraft jet noise on the community, the effect of flight on the jet exhaust noise must be assessed and be predictable. While it is well known that jet noise associated with conical nozzles is reduced by flight speed, conflicting acoustic results have been obtained with suppressor nozzles. Indeed, for the most part, little reduction in suppressor nozzle jet noise with flight speed has been obtained.

Measured inflight jet noise data have been published in the open literature for only a limited number of nozzle configurations. These latter include conical, 8-lobed, and 104-tube nozzles.[1,2]

A much larger data base of simulated flight effects on both unsuppressed and suppressed nozzle configurations has been compiled at model scale. Most of these data have been generated as part of the comprehensive FAA/DOT program with the General Electric Company. This program concentrated on high velocity jet noise source location and reduction (DOT-OS-30034) using a free jet as a flight simulation facility. The author is grateful for the cooperation of the cognizant contract officers at FAA (Mr. R. S. Zuckerman) and GE (Mr. V. L. Reed) in releasing some of the data for inclusion herein. Finally, simulated flight acoustic data obtained with engines as well as scale-model nozzles in the NASA Ames 40- by 80-foot wind tunnel are contained in the data bank.[3,4]

The purpose of this paper is to provide an assessment of and an insight into the inflight acoustic performance of a variety of jet noise suppressor nozzles. The suppression of jet noise over the entire range of directivity angles is of general interest (Fig. 1). However, for supersonic aircraft, the jet exhaust noise in the rear quadrant is of particular interest because the rotation angle of the aircraft during takeoff and approach is very high compared with present subsonic aircraft. Consequently, this paper will consider primarily the flight effects at the peak perceived noise level (PNL) angle associated with suppressor nozzle configurations (nominally $\theta \sim 130^{\circ}$).

Photographs of some of the suppressor nozzles considered herein are shown in Figs. 2 and 3.

The model scale acoustic data used in this paper were scaled up, in the references, to an "engine" nozzle exhaust total area of 2181 cm^2 (J-79 engine size) and to a sideline distance of 732 m. For this study, most of the model scale data used are for a nominal jet velocity (mixed or single stream) of about 701 m/sec, except where noted.

Background

Inflight

Perceived noise level. A comparison of static and inflight PNL as a function of directivity angle is shown schematically in Fig. 1. The figure represents typical inflight effects on jet exhaust noise for a conical nozzle operating with supersonic flow. It is apparent that the noise in flight is significantly reduced from the static condition in the rear quadrant, particularly near the peak PNL angle.

Jet noise reduction in flight is a function of three factors:

(1) A source alteration
(2) A kinematic effect
(3) A dynamic effect

Detailed equations for these terms are given in Ref. 5. The static noise level is reduced in flight by the summation of these three terms. At $\theta = 90^{\circ}$, only the source is altered by forward velocity. In the forward quadrant, the source term and the combined kinematic and dynamic terms act in opposition to each other. The combined kinematic and dynamic terms can be expressed for a close approximation to the exact values by 40 log $(1 - M_o \cos \theta)$. This simplified expression, defined as the moving medium effect, is used herein for convenience in later comparison calculations of inflight effects on suppressor nozzle jet noise. Similarly, the source alteration is simplified, for the purposes herein, to 50 log $(1 - V_o/V_j)$.

Spectra. The effect of flight on jet noise spectra near the peak PNL angle is shown in Fig. 4. The spectra shown were obtained from inflight studies with a General Dynamics F-106 using a J85-13 engine[1,2] and a Gates - Learjet using a civilian derivative of the J85 engine.[2] The spectra shown in Fig. 4 include conic (baseline) nozzles and two suppressor nozzles, an 8-lobe nozzle and a 104 tube nozzle. The spectrum for each nozzle shows a decrease in SPL level at all frequencies with flight. The amount of SPL reduction due to flight depends, in the absence of other noise sources, such as core noise, on the type of nozzle, magnitude of the jet velocity, and flight velocity.

Flight Simulation

The effect of flight on jet noise has been measured in both wind tunnels and free jet facilities. The measured acoustic data from each of these facilities require a correction or transformation when compared with flight data.

Wind tunnel data. Data obtained in acoustic wind tunnels (microphones mounted within the free stream) show PNL or spectral source reductions of about equal magnitude at all angles. These data, however, require both a moving medium correction to the measured PNL or spectral data and a frequency shift.[4]

Free jet data. Model-scale spectra for a conical nozzle obtained in a free jet flight simulation facility[6] are shown in Fig. 5 for a static and flight simulation case. The spectra shown are for the peak PNL angle ($\theta = 130^{o}$).

The measured flight-simulated jet noise requires both the moving medium correction and, because the microphones are located outside the free jet boundaries, a shear layer correction. For the data reported in Refs. 7 to 10 transformation procedures have been developed to achieve these corrections. These transformations result in a reduction of the flight simulated spectrum level from the measured SPL values as indicated in Fig. 5, taken from Ref. 6. The transformed flight simulation spectrum then exhibit similar trends and SPL magnitudes with forward velocity, relative to the static spectrum, to those observed previously for the inflight spectra shown in Fig. 4.

The transformation procedures from Refs. 7 and 8 are somewhat similar in concept and yield similar results. However, the procedure developed for the data in Refs. 9 and 10 includes a turbulence absorption parameter that is not included in the procedures of the other two references. Initially, this parameter attained a peak value of 6 dB at the higher model-scale frequencies and was angle dependent through an additive procedure.[9] Subsequently, the peak value was reduced to 3 dB.[10] Presently (unpublished NASA contractual work) the peak value of 3 dB has been retained; however, the variation with directivity angle is now a multiplication factor rather than an additive factor. In Figs. 6 and 7 are shown the static measured data and the transformed flight simulation spectra with and without the turbulence absorption parameter for a conical nozzle and a 104 tube suppressor nozzle.[9] The removal of the turbulence absorption effect is approximate due to the nature of the procedures; this correction was made prior to the dynamic transformation. The spectra shown are the for engine size. Considering the flight effects shown in Fig. 4, the transformed flight simulation data without the turbulence absorption parameter appear to represent the trends and magnitude variations with forward velocity much better than with this parameter, particularly at the higher frequencies. Consequently, the transformed spectral data from Refs. 9 and 10 have been adjusted herein by the approximate deletion of the turbulence absorption parameter. The better agreement resulting from deletion of this turbulence absorption parameter suggests that the transformation procedures used in Refs. 9 and 10 should be reexamined in order to validate the absolute spectral SPL levels for the flight-simulated data in the absence of this factor.

Suppression Mechanisms

Static

An excellent discussion is given in Ref. 11 on suppression mechanisms applicable to suppressor nozzles under static operation. As stated in Ref. 11, the noise reduction characteristics of a suppressor nozzle are intimately associated with a rapid mean-velocity decay of the exhaust plume. This rapid velocity decay is caused by the breakup of the exhaust plume into many discrete flow elements by the multielements of the suppressor nozzle. A schematic sketch of the pertinent aero-acoustic relationships of flow region, suppressor nozzle, spectrum, and exhaust plume velocity decay is shown in Fig. 8. The exhaust plume consists of two major flow regimes, the premerged and the merged flow regions. The premerged flow region is that portion of the plume directly downstream of the nozzle exhaust plane where the flow issuing from a multielement suppressor nozzle consists of distinctly individual streams. The merged flow region, farther downstream of the nozzle exhaust plane, is that portion of the plume where the flow from the individual nozzle elements has merged into a single large stream similar to that for a conical nozzle. The usual suppressor nozzle (spoke, chute, tube, etc.) spectrum in the literature has a Bactrian (two hump) spectral shape compared with the Dromedarian (one-hump) spectral shape of a conical nozzle spectrum. The low frequency portion of the spectrum, as shown in Fig. 8, is associated with the downstream merged flow region. The high frequency portion of the spectrum is associated with the individual jet streams created by the suppressor elemental nozzles in the premerged flow region. The relative peak level between these two flow regions is a function of the suppressor nozzle design.

The plume velocity decay shown in Fig. 8 is also related to the flow regions. In the premerged flow region, the local jet velocity is maintained at or near the jet exhaust velocity. In the merged flow region, the plume velocity has decayed to a much lower average velocity, generally of the order of 50 to 75 percent of the initial jet exhaust velocity, depending on the suppressor nozzle design.

The rapid plume velocity decay for suppressor nozzles suggests that the noise producing eddies in the plume are convected downstream at much lower velocities than in a conical nozzle case.[11] This should result in the best noise reduction being achieved by suppressor nozzles that produce the most rapid plume decay and, hence, lowest convection

velocities. The nozzle design factors that promote static noise reduction include both larger numbers of suppressor elements and discrete element area ratio in order to promote more rapid plume velocity decay. Finally, it is concluded in Ref. 11 that multielement suppressors do not reduce the turbulent mixing noise but instead redistribute it to higher frequencies. At these higher frequencies atmospheric attenuation can reduce this effect thereby lowering the noise transmitted from the source to the observer. The convective amplification is reduced with multielement suppressor nozzles because of the reduction in the plume velocities; however, this is offset to some extent by a loss in fluid shielding. Although not pertinent to this study, which concentrates on the peak PNL angle, suppressor nozzles also reduce forward quadrant shock noise compared with that for conical nozzles. Here, the small discrete nozzles of a suppressor nozzle cause the shock cell spacing and cross sections to be smaller and possibly fewer in number, resulting in lower noise production at higher frequencies.[11]

Flight

When flight effects (forward velocity) on multielement suppressor nozzle noise are considered, the static spectrum and plume velocity decay curves are altered as shown schematically in Figs. 9(a) and (b), respectively. The largest inflight noise reduction occurs in the merged flow region (low frequencies, downstream portion of plume). The SPL levels decrease with increasing forward velocity. At the same time, the velocity at a given axial distance from the nozzle exhaust plane, X/D_e, increases with forward speed.[12] These differences in SPL reduction for the two flow regions will be discussed later herein. For a rigorous analysis of the flight effects on the jet noise spectrum, information on the plume velocity decay must be related to the frequency content of the spectrum. Through multiple sideline measurements[13] or other techniques (such as acoustic mirrors[2]) the necessary spectral information can be obtained. An example of this type of information is shown in Fig. 9(c) in which the Strouhal number, given by $fD_e/V_j - V_o$ is plotted as a function of noise source location, X/D_e. The curve represents typical information for a supersonic jet exhaust velocity.[14] Finally, the relation of the spectral frequency to the local plume velocity is shown in Fig. 9(d). From this latter information and appropriate source alteration calculation procedures, analogous to those discussed in Ref. 5, the flight effects on the local spectral SPL's can be obtained.

Measured Spectral Flight Effects

The flight effects on the jet noise at $\theta = 90^\circ$ and 130° (approx. peak PNL angle) for several model-scale suppressor nozzles are examined. The nozzles are divided into two categories, single stream and dual stream.

90° Directivity Angle

Single stream nozzles. The spectra for two single stream nozzles are shown in Fig. 10. In general, reductions in SPL are obtained in flight in the merged flow region of the spectra. This flow region for the nozzle size herein contain frequencies generally less than 630 Hz. The amount of suppression due to flight effects in the merged flow region varies with the particular suppressor design; the highest suppression being associated with the largest plume velocity decay.[11] The high frequency is little affected by forward velocity. From this it is apparent that the source alteration due to flight effects is obtained only, or at least mainly in the merged flow region of the jet; that is, at low frequencies for the engine size used in this paper. In the premerged flow region, the pumping action of the individual nozzle streams induces an outside airflow around each of the multielement flows. This induced airflow constitutes a pseudo forward velocity effect on the individual element streams which is included in the static SPL measurements. Consequently, in the flight case no further noise reduction is afforded by forward velocity at normal takeoff or landing speeds.

Dual stream nozzles. The spectra for several dual stream suppressor nozzles are shown in Figs. 11 and 12. The suppressor nozzles for which the data are shown in Fig. 11 consisted of coannular inverted velocity-profile nozzles (higher jet velocity in outer stream than that in inner stream) with outer stream suppressors. The spectra, taken from Ref. 10, as in the case of the single stream suppressor nozzles show little noise reduction in the premerged flow region. In the merged flow region, significant SPL reductions are obtained. From these data it is evident that the source alteration due to flight is again confined primarily to the merged flow region.

The flight effects on the spectrum of a 54-element coplanar mixer nozzle are shown in Fig. 12. In this nozzle design, the core and fan streams efflux from alternating adjacent nozzle elements. It is evident from the spectra that a source alteration is achieved over the entire frequency range; that is, over both premerged and merged flow regions. The SPL reductions due to flight effects is substantially similar in trend to that for a conical nozzle.

130° Directivity Angle

Single stream nozzles. The effect of flight on suppressor nozzles is shown in Fig. 13 for the peak PNL angle ($\theta = 130^\circ$). In all cases, the merged flow region ($f \lesssim 630$ Hz) shows much larger SPL suppressions than those at $\theta = 90^\circ$. This results from a combined source alteration and the moving medium effects. In addition, the premerged flow region also indicates suppressed SPL values. These SPL suppressions in the permerged flow region (Fig. 8) are due to the moving medium term (approximated herein by 40 log $(1 - M_o \cos \theta)$), and amount to from 2.5 to 3.5 dB for V_o values of 84 and 110 m/s, respectively. Actually the moving medium effects, which depend on source convection velocity should differ somewhat for the merged and premerged regions. The variation in SPL suppression in the merged flow region and its significance on PNL will be discussed in more detail later herein.

Dual stream nozzles. The flight effects on the spectra at $\theta = 130^\circ$ for two dual stream multielement suppressor nozzles are shown in Fig. 14. In general, the flight effects are similar to those noted for the single-stream nozzles.

The flight effects on a multielement coplanar mixer nozzle are shown in Fig. 15. As in the case of $\theta = 90^{o}$, the flight effects suppress the entire spectrum, with substantially, equal SPL reductions at all frequencies. This indicates that a source alteration occurs over the entire spectrum together with reductions due to the moving medium effect. It should be noted that the SPL reductions due to forward velocity with this nozzle exceed those for a conical nozzle with the same maximum exhaust velocity (790 m/s). The larger SPL suppression is attributed to the mixing between the adjacent high/low flow nozzle elements enhanced by interaction with the flight velocity.

Merged-Flow Noise Source Alteration Due to Flight

The noise source alteration due to flight in the merged flow region can be obtained from Ref. 5 and can be approximated closely for the present purposes by 50 log $(1 - V_o/V_c)$ where V_c is the local centerline or mean jet velocity in the plume in the merged flow region (Fig. 9(b)) instead of V_j. From this equation the average or local velocities in the merged flow region can be estimated from the spectral data. For the nozzles herein, the following average merged flow velocities based on the spectral static-to-flight differences at $\theta = 90^{o}$ were calculated according to the preceding equation:

Reference	Nozzle	Type	Calculated merged flow region average velocity, V_c, m/s	V_c/V_j	V_c/V_{jo}	V_c/V_m
9	104-tube	Single flow	479	0.66	----	----
9	32-chute	Single flow	362	.52	----	----
10	40-shallow chute	Dual flow	523	----	0.67	0.75
10	36-chute	Dual flow	345	----	.44	.49
10	54-element mixer	Dual flow	476	----	.60	.68

The preceding calculated jet velocities and velocity ratios are of the same order as might be expected from plume velocity decay data given in Refs. 11, 12, and 15 for similar nozzle configurations and flow conditions. It follows from this exercise, that the reverse procedure can be used to calculate the ΔSPL_S when the plume velocity decay information for the merged flow region is available.

The moving medium effect becomes zero at $\theta = 90^{o}$ for both the merged and premerged flow regions and, as discussed previously, only the source term, SPL_S, in the merged flow region is altered by forward velocity. For the suppressor nozzles herein, except for the 54 element coplanar mixer nozzle, the sum of the ΔSPL_S at $\theta = 90^{o}$ (Figs. 10 and 11) and the ΔSPL_M at each frequency in the merged flow region when subtracted from the SPL_{STAT} at $\theta = 130^{o}$ should yield the SPL_{FLT} at $\theta = 130^{o}$. The validity of this procedure is shown in Figs. 16 and 17. Except for the 36-chute nozzle (Fig. 17(b)) agreement between the "calculated" and measured SPL SPL values at $\theta = 130^{o}$ in the merged flow region is good.

Summary of Flight Effects on Suppressor Nozzle Noise at Peak PNL Angle

The flight effects on the jet spectrum at the peak PNL angle can be summarized as follows:

1. The local SPL values with multielement suppressor nozzles are reduced inflight over the entire frequency spectrum, but more so in the downstream merged flow region than in the premerged flow region. In the case of a multielement mixer nozzle, the local SPL values in flight are lowered nearly equally at all frequencies.

2. With multielement suppressor nozzles, the SPL in the premerged flow region is reduced in flight only by the moving medium effects with no source alteration (reduction). The SPL in the merged flow region, however, is reduced inflight by both a source alteration and the moving medium effect.

3. An increase in jet velocity, either V_j for a single-stream suppressor nozzle or V_{jo} for a dual-stream suppressor nozzle (coannular IVP type nozzle with outer stream suppressor), increases the merged flow SPL relative to that for the premerged flow region. (Not shown herein[10].)

4. With a coannular IVP suppressor nozzle decreasing the inner flow velocity, V_{ji}, with constant outer flow velocity, V_{jo}, causes an increase in source alteration in flight. (Not shown herein, unpublished NASA data.)

5. Increasing the inflow velocity between the individual jet streams in the premerged flow region of a suppressor, as with the 54-element coplanar mixer nozzle, causes large static source alterations and consequent significant noise reductions that are maintained or even amplified in flight.

Effect of Spectral Shape on PNL

The measured data in the preceding section of this paper have shown that for suppressor nozzles inflight source alteration occurs only for the merged flow region. Note that this conclusion does not apply to the 54 element coplanar mixer nozzle. Consequently, the effect of changing the magnitude of the merged flow SPL source alteration on the PNL is now further examined.

In order to assess the effect of suppressing the SPL's in the merged flow region on the total peak PNL, three static spectra representative of typical suppressor nozzles were examined. These

spectra, shown in Fig. 18, are labeled A, B, and C. Spectrum A represents nozzles having significantly higher static SPL values in the merged flow region than in the premerged flow region. For the selected spectrum, the peak SPL level in the merged flow region was 8 dB higher than that in the premerged region. Spectrum B represents suppressor nozzles having equal peak SPL values in the merged and premerged flow regions. Finally, spectrum C represents suppressor nozzles having a 5 dB lower peak SPL value in the merged flow region than that in the premerged flow region. The absolute SPL levels for the three spectra are of the same order of magnitude as those shown in Refs. 9 and 10 and are based on a total nozzle exhaust area of 2181 cm^2, a jet exhaust velocity of 701 m/s and for a sideline distance of 732 m.

Peak PNL Angle, $\theta = 130^o$

The flight spectra for the three representative static spectra are shown in Fig. 19. As discussed previously, the flight effects on the SPL at the peak PNL angle reduce the static values by both a source alteration and a moving medium effect. In Fig. 19, the static data are reduced by a moving medium effect of -3.5 dB (due to a forward velocity of 122 m/s) and arbitrary merged flow region source alterations of -5 and -10 dB. Thus, summing ΔSPL_s and ΔSPL_M, total suppressions of -8.5 and -13.5 dB are obtained in the merged flow region. In the premerged flow region, the flight effect consists only of the moving medium effect which, in flight, reduces the static SPL by -3.5 dB. In all cases this latter flight effects suppression was calculated by 40 log $(1 - M_o \cos \theta)$.

The inflight PNL reductions are summarized in the following table:

Spectral shape	ΔPNL due to flight effects, PNdB		
	Merged flow region ΔSPL_s, dB	-5	-10
A		-5.4	-6.8
B		-4.9	-5.9
C		-4.4	-5.0

Of the total ΔPNL listed in the preceding table, -3.5 dB was contributed by the moving medium effect which applied at all frequencies. The contribution of the merged flow region source alteration is assessed by $\Delta PNL - \Delta PNI_M$ in the following table:

Spectral shape	$\Delta PNL - \Delta PNI_M$, PNdB		
	Merged flow region ΔSPL_s, dB	-5	-10
A		-1.9	-3.3
B		-1.4	-2.4
C		-.9	-1.5

The spectral shape for most suppressor nozzles at the peak PNL are represented by the A-shape of Fig. 19, with the ΔSPL peaks for the two flow regions, varying from 3 to 10 dB. Thus, at the peak PNL angle, the merged flow region source alteration due to flight influences the PNL suppression by about 1/2 to an equal amount (in dB) of the suppression due to the moving medium effects for the assumed conditions of $V_j = 701$ m/s and $V_o = 122$ m/s.

If the turbulence absorption factor had been retained, the SPL levels in Figs. 10 to 15 would be increased, by at least 3 dB in the higher frequency range. This would emphasize the fact that the premerged flow region is the dominant noise source. When the PNL is calculated for a particular nozzle, the noise weighting factors maximize in the frequency range associated with the premerged flow region. A change in engine-scale nozzle size would not significantly alter the fact that the premerged flow region generally constitutes the dominant noise source for sideline PNL considerations.

In the following two sections, the flight effects on the PNL at $\theta = 90^o$ and in the forward quadrant, $\theta = 50^o$, are briefly considered.

90° Directivity Angle

As previously shown in Figs. 10 and 11 at $\theta = 90^o$ only the merged flow region has a source alteration due to forward velocity. Also, at this angle the moving medium effect, ΔSPL_M, is zero. In Fig. 20, are shown the same three static spectral shapes that were used to examine the effect of forward velocity on the spectra and PNL at $\theta = 130^o$. Also shown are the spectral shape variations for merged flow source alterations of -5 and -10 dB. The inflight PNL reductions caused by these source alterations are the same as those listed in the preceding table in which the $\Delta PNL - \Delta PNI_M$ is given. From these calculations it is obvious that large source alterations (ΔSPL_s) in the merged flow region do impact the PNL for a nozzle significantly. For the suppressor nozzles shown in Figs. 2 and 3, the impact of ΔSPL_s on the PNL for these nozzles amounts to less than 2 PNdB and, in most cases, more like 1 PNdB. For $\theta = 90^o$, spectral shape A is representative of the acoustic results obtained from a suppressor nozzle such as the 104-tube suppressor nozzle (Fig. 2(a)) while spectral shapes B and C represent those shown in Figs. 2(b) and 3(a) and (b).

Forward Quadrant, $\theta = 50^o$

In the forward quadrant, the moving medium effect increases the local SPL, hence the PNL, compared to the static value. At the same time, the source alteration decreases the local SPL and, hence, the PNL. In Fig. 21 are shown the same three static spectral shapes used previously for $\theta = 90^o$ and 130^o. At $\theta = 50^o$ with forward velocity, the moving medium effect, ΔSPL_M increases the static SPL by +3.5 dB ($V_o = 122$ m/s) over the entire spectra. Source alterations due to forward velocity of -5 and -10 dB are then applied to the $SPL_{STAT} + \Delta SPL_M$ in the merged flow region, resulting in the inflight spectral shapes shown in Fig 21. The PNL variations caused by these inflight effects on the spectra are summarized in the following table:

Spectral shape	ΔPNL due to flight effects, PNdB		
	Merged flow region ΔSPL_8, dB	-5	-10
A		+1.6	+0.1
B		+2.0	+1.1
C		+2.7	+2.2

It is apparent from this table that the moving medium effect dominates the flight effects, even with a source alteration of -10 dB in the merged flow region.

At $\theta = 50^0$, spectral shape A is representative of a suppressor nozzle such as the 104 tube nozzle (Fig. 2(a)) while spectral shapes B and C are representative of suppressor nozzles such as shown in Figs. 2(b) and 3(a) and (b).

Considerations for Future Suppressor

Nozzle Designs

On the basis of the data and acoustic trends shown by the suppressor nozzles included herein, a number of possibilities appear feasible for improving the noise reduction effectiveness of suppressor nozzles for supersonic cruise aircraft.

The 54-element coplanar mixer nozzle acoustic results suggest that if the naturally induced flow between suppressor nozzle elements produced by the pumping action of the individual nozzle streams is augmented or replaced by forced flow, the premerged flow region at the peak PNL angle (as well as other directivity angles) will respond to flight effects. This noise source then will be reduced in a manner similar to that for the merged flow region noise source. In addition, because the mixed local jet velocity is less than the peak jet velocity, the flight effects will be increased over that with a conical nozzle. The flow between these jets perhaps could be implemented for a turbojet engine by providing long external airflow channels upstream of the nozzle exhaust plane or providing better pumping action by introducing compressor bleed air into the region between the jets, thereby promoting more rapid mixing of the multielement jets with the surrounding air. For a low-bypass engine, the fan flow could be exhausted between the core engine multielement nozzles and jets. For the VCE-IVP nozzles, a portion of the inner stream (fan flow) could be channeled to provide the required mixing with the outer stream in a modified mixer-type suppressor nozzle.

The 54-element coplanar mixer nozzle meets most of the preceding needs for good suppressor nozzle design; however, it does have some shortcomings in performance. In particular, the peak static PNL is too high relative to that of a conical nozzle. In addition, the peak static suppression occurs at a lower jet velocity than that desired for supersonic cruise aircraft application. However, this shortfall perhaps can be surmounted by changes in the aspect ratio and/or number of the nozzle elements.

A comparison of the spectra for the 54-element coplanar mixer nozzle with that for a coannular inverted-velocity-profile suppressor nozzle (36 chute nozzle configuration) is shown in Fig. 22 for $\theta = 90^0$ and 130^0. The data shown are for nearly the same V_{j0} although the V_{j1} are somewhat different. Both inflight sets of data are for a flight velocity of 110 m/s. At $\theta = 90^0$, the static spectrum for the mixer and chuted suppressor nozzles are somewhat similar with the mixer nozzle having higher SPL values in the 315 to 1250 Hz frequency range and lower SPL values at frequencies greater than 2000 Hz range than those for the chuted nozzle. The inflight spectra, however, indicate that the SPL's for the mixer nozzle are significantly less for frequencies over 1000 Hz than those for the chuted nozzle. This results in an inflight PNL reduction of 2.8 PNdB for the mixer nozzle compared with the 36-chute nozzle.

At $\theta = 130^0$, the static SPL values for the mixer nozzle are substantially higher than those for the 36 chute suppressor nozzle over the greater portion of the spectra. In terms of PNL, the mixer nozzle PNL is 4.4 dB higher than that for the chute suppressor nozzle. However, the inflight spectra for the two nozzles show trends similar to those noted for $\theta = 90^0$. The mixer nozzle PNL is 1.6 dB less than that for the chute suppressor nozzle.

In summary then, future suppressor nozzles for supersonic cruise aircraft should include the following design criteria in order to provide maximum jet noise suppression:

(1) The high frequency regime associated with the premerged flow region should be provided with an augmented flow between the high velocity nozzle elements. This provision yields a source alteration in flight with a consequent noise suppression.

(2) The PNL of the premerged flow region is the dominant noise source for most practical suppressor nozzles; consequently, the level for this noise source should be minimized, again within acceptable thrust performance, by suitable design of the individual nozzle elements with respect to element aspect ratio and number.

(3) The axial velocity decay of the jet stream should be rapid and to as low a velocity as feasible while maintaining a high thrust level. This provides a low noise level for the merged flow region (low frequency regime).

Concluding Remarks

The data herein and that in the references, suggest a possible method for estimating the flight effect on engine-size jet suppressor nozzle noise on the basis of spectral changes. In the merged flow region (low frequencies), the static-to-flight source noise suppression can be estimated by use of plume velocity decay data and the source alteration methods of Ref. 5 applied to the spectrum. For the premerged flow region, no source alteration occurs for conventional suppressor nozzles (spoke, chute, tube, etc.). A moving medium effect applies to both flow regions. Use of an ejector with acoustically treated walls is probably the most effective means to reduce the premerged flow region noise levels. Such an ejector must be sized and designed for the supersonic cruise condition, but must also perform well in any subsonic portion of the aircraft mission. In the latter operational mode,

which includes take-off, an ejector usually is subject to aerodynamic performance penalties. An ejector, with its associated controls, also tends to penalize the aircraft range due to its added weight. The offsetting effects of an ejector system require a careful trade-off study in order to ascertain its optimum environmental/performance benefits.

For novel suppressor nozzles, such as the multielement coplanar mixer type, the source alteration due to flight extends over all the frequency bands. Thus, the source alteration due to flight, as obtained from Ref. 5 is coupled with the plume velocity decay over both the merged and premerged flow regions. As in the case of conventional suppressor nozzles the moving medium effect is applied to the entire spectrum.

In summary, the effect of flight on the spectra of suppressor nozzles of the type using spokes, chutes, tubes, etc. as herein can be estimated to a first order approximation from the following equations:

(a) Merged flow region

$$SPL_{FLT} = SPL_{STAT} - \Delta SPL_M + \Delta SPL_s$$

(b) Premerged flow region

$$SPL_{FLT} = SPL_{STAT} - \Delta SPL_M$$

where

$$\Delta SPL_M = 40 \log (1 - M_o \cos \theta)$$

and

$$\Delta SPL_s = 50 \log (1 - V_o/V_c)$$

More exact SPL variations due to flight effects can be obtained by the use of the more complex relationships involving the kinematic, dynamic, and source alteration given in Ref. 5.

For a multielement coplanar mixer type suppressor nozzle it appears that the preceding SPL relationship for the premerged flow region applies over the entire spectrum. However, further work is needed to verify this conclusion.

Appendix

Symbols

AR	suppressor area ratio; total suppressed nozzle area, excluding plug, divided by suppressed nozzle flow area
D_e	equivalent diameter
f	1/3-octave band center frequency
M_o	flight Mach number
PNL	perceived noise level, PNdB
SPL	1/3-octave band sound pressure level, dB re 20 $\mu N/m^2$
V	jet exhaust velocity
V_o	forward or free stream velocity
X	axial distance downstream of nozzle exhaust plane
Δ	difference
θ	directivity angle referred to inlet axis

Subscripts:

c	centerline
D	dynamic effect
FLT	flight
j	jet
ji	inner stream jet
jo	outer stream jet
K	kinematic effect
l	local
M	moving medium effect
m	mean
s	source
STAT	static

References

1. Burley, R. R., "Flight Velocity Effects on the Jet Noise of Several Variations of a 104-Tube Suppressor Nozzle," NASA TM X-3049, 1974.

2. Clapper, W. S. and Stringas, E. J., "High Velocity Jet Noise Source Location and Reduction, Task IV-Development/Evaluation of Techniques for "Inflight" Investigation," General Electric Co., Cincinnati, Ohio, R77AEG189, Feb. 1977. (FAA-RD-76-79-4; AD-A041849).

3. Stone, J. R., Miles, J. H., and Sargent, N. B., "Effects of Forward Velocity on Noise for a J85 Turbojet Engine with Multi-Tube Suppressor from Wind Tunnel and Flight Tests," NASA TM X-73542, 1976.

4. Jaeck, C. L., "Static and Wind Tunnel Near-Field/Far-Field Jet Noise Measurements from Model Scale Single-Flow Baseline and Suppressor Nozzles, Volume 2 - Forward Speed Effects," Boeing Commercial Airplane Co., Seattle, Wash., D6-44121-2-VOL-2, Nov. 1976. NASA CR-137914.

5. Stone, J. R., "An Improved Method for Predicting the Effects of Flight on Jet Mixing Noise," NASA TM-79155, 1979.

6. Packman, A. B., Ng, K. W., and Patterson, R. W., "Effect of Simulated Forward Flight on Subsonic Jet Exhaust Noise," AIAA Paper 75 869, June 1975.

7. Ahuja, K. K., Tester, B. J., and Tanna, H. K., "The Free Jet as a Simulator of Forward Velocity Effects on Jet Noise," NASA CR-3056, 1978.

8. Amiet, R. K., "Correction of Open Jet Wind Tunnel Measurements for Shear Layer Refraction," AIAA Paper 75-532, Mar. 1975.

9. Clapper, W. S., Baumgardt, N., Brausch, J. F., Mani, R., Stringas, E. J., Vogt, P., and Whitaker, R., "High Velocity Jet Noise Source Location and Reduction," Task III - Experimental Investigation of Suppression Principles, Vol. 2 - Parametric Testing and Source Measurements," Federal Aviation Administration, Washington, D.C., FAA-RD-76-79, III-II, May 1978.

10. Clapper, W. S., Baumgardt, N., Brausch, J. F., Mani, R., Stringas, E. J., Vogt, P., and Whitaker, R., "High Velocity Jet Noise Source Location and Reduction," Task V - Investigation of 'In-Flight' Aeroacoustic Effects on Suppressed Exhausts," Federal Aviation Administration, Washington, D.C., FAA-RD-76-79, V, July 1978.

11. Gliebe, P. R., "Diagnostic Evaluation of Jet Noise Suppression Mechanisms," AIAA Paper 79-0674, Mar. 1979.

12. von Glahn, U., Groesbeck, D. E., and Goodykoontz, J. H., "Velocity Decay and Acoustic Characteristics of Various Nozzle Geometries with Forward Velocity," NASA TM X-68259, 1973.

13. Stone, J. R., Goodykoontz, J. H., and Gutierrez, O. A., "Effects of Geometric and Flow-Field Variables on Inverted-Velocity-Profile Coaxial Jet Noise and Source Distributions," NASA TM-79095, 1979.

14. Moore, M. T., "Flight Effects on the Jet Noise Signature of a 32-chute Suppressor Nozzle as Measured in the NASA Ames 40×80 Foot Wind Tunnel," General Electric Co., Cincinnati, OH, Jan. 19[illegible], NASA CR-152175.

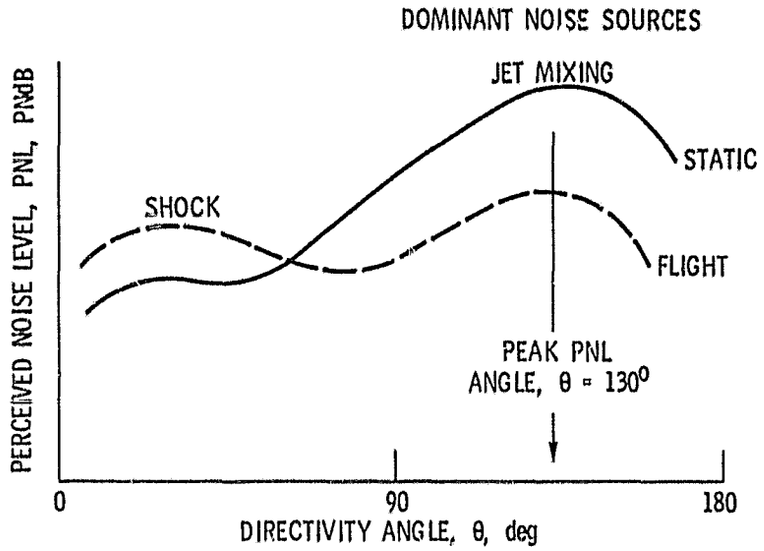

Figure 1. - Comparison of typical static PNL with flight PNL as a function of directivity angle. Supersonic jet velocity.

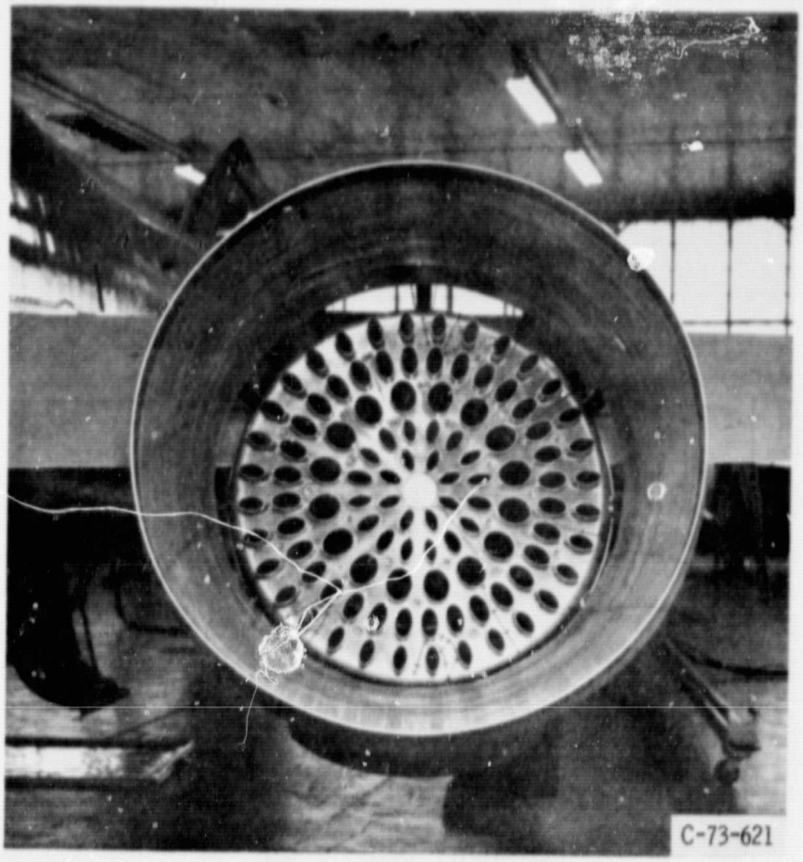

(a) 104-TUBE SUPPRESSOR NOZZLE ON F-106 AIRCRAFT. REF. 4.

Figure 2. - Photographs of typical single-stream suppressor.

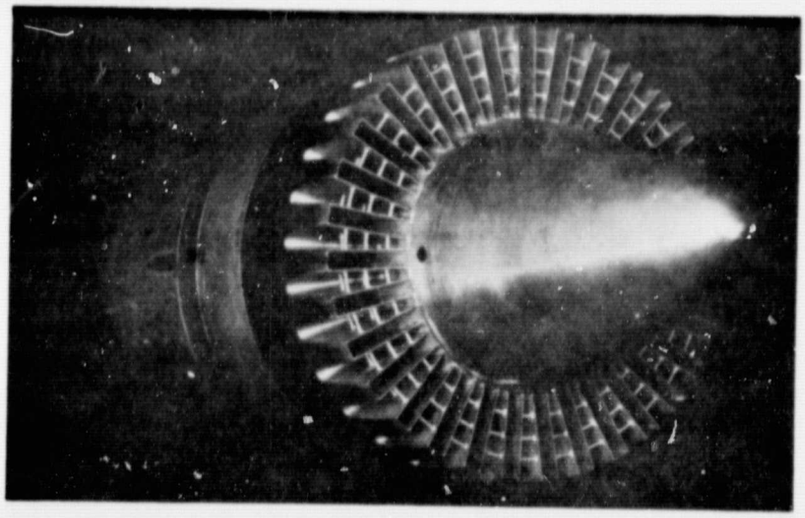

(b) 32 CHUTE SUPPRESSOR NOZZLE. REF. 10.

Figure 2. - Concluded.

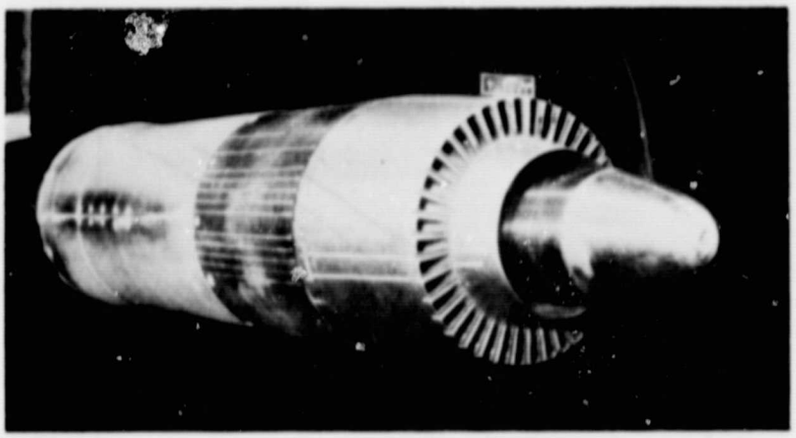

(a) 40-SHALLOW CHUTE NOZZLE.

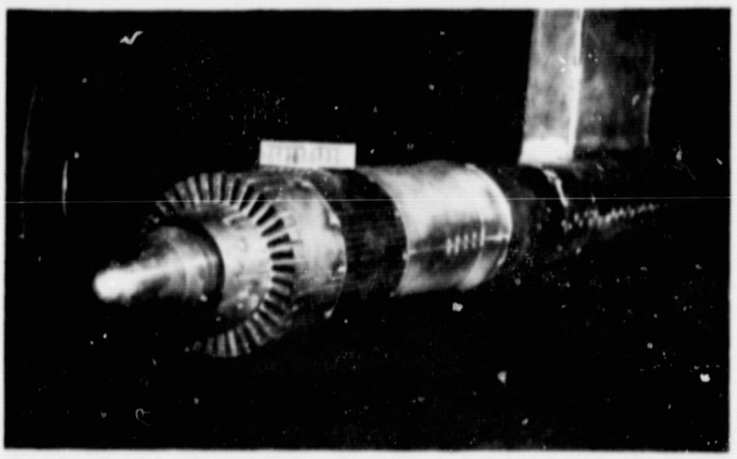

(b) 36-CHUTE NOZZLE.

Figure 3. - Photographs of typical dual-stream suppressor nozzles. REF. 10.

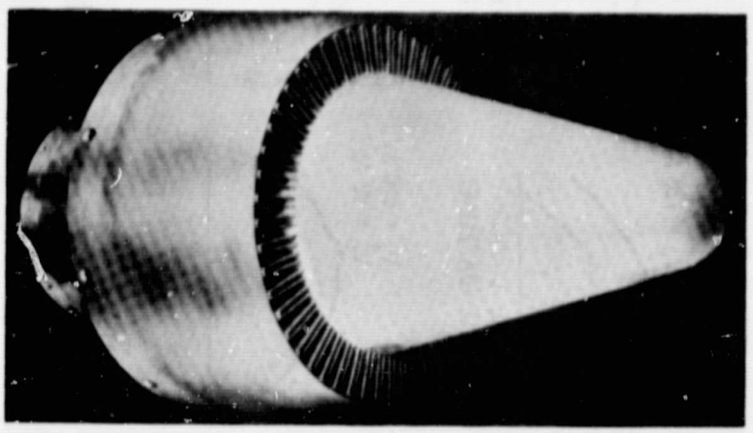

(c) 54-ELEMENT COPLANAR MIXER NOZZLE.

Figure 3. - Concluded.

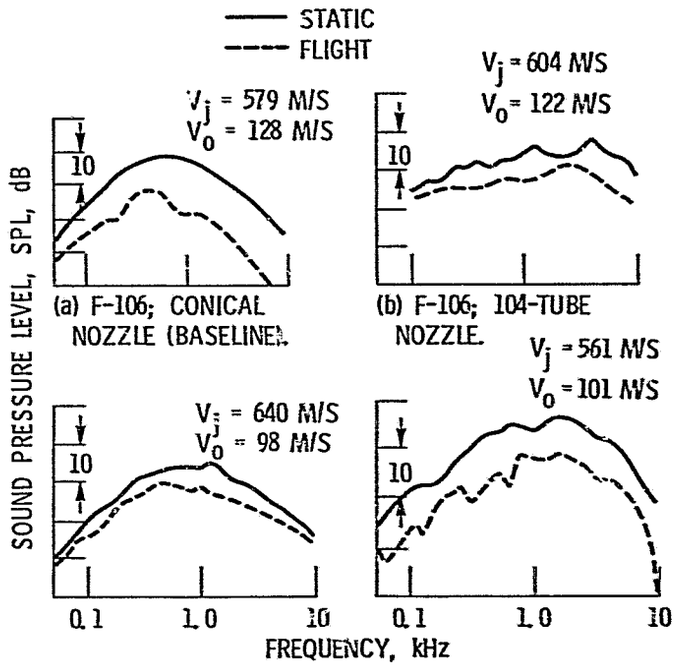

(a) F-106; CONICAL NOZZLE (BASELINE).

(b) F-106; 104-TUBE NOZZLE.

(c) GATES-LEARJET; CONICAL NOZZLE.

(d) GATES-LEARJET; 8-LOBE NOZZLE.

Figure 4. – Comparison of measured static and flight spectra at peak PNL angle ($\theta = 130^0$) for several nozzle types. 122 m sideline distance; reference 2.

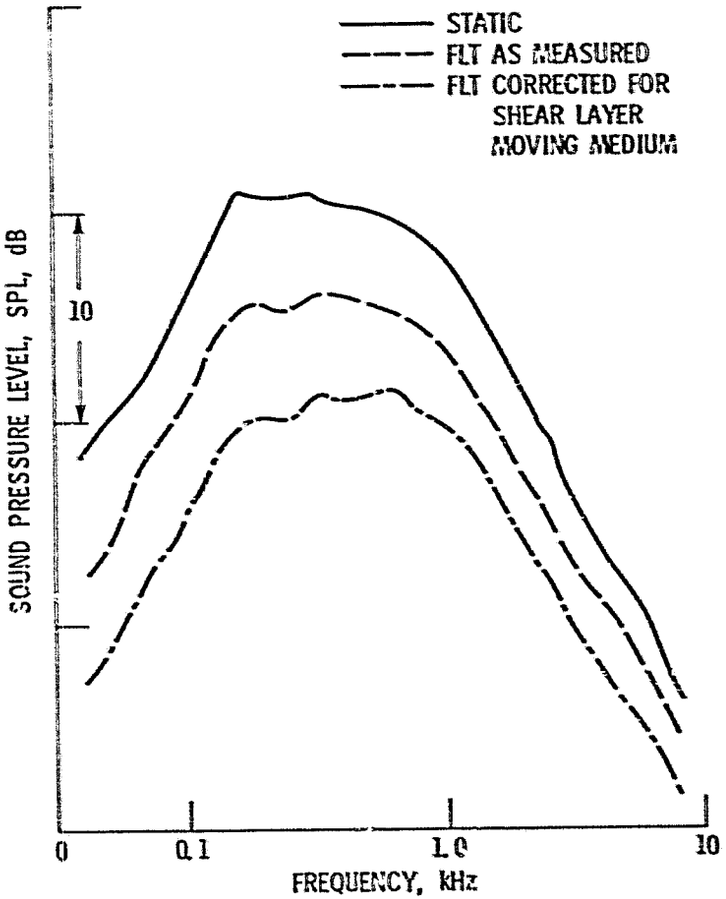

Figure 5. – Comparison of model-scale static and free-jet facility flight simulation spectra at peak PNL angle ($\theta = 130^0$). Jet velocity, V, 509 M/S; data taken at 3.05 m radius; reference 6.

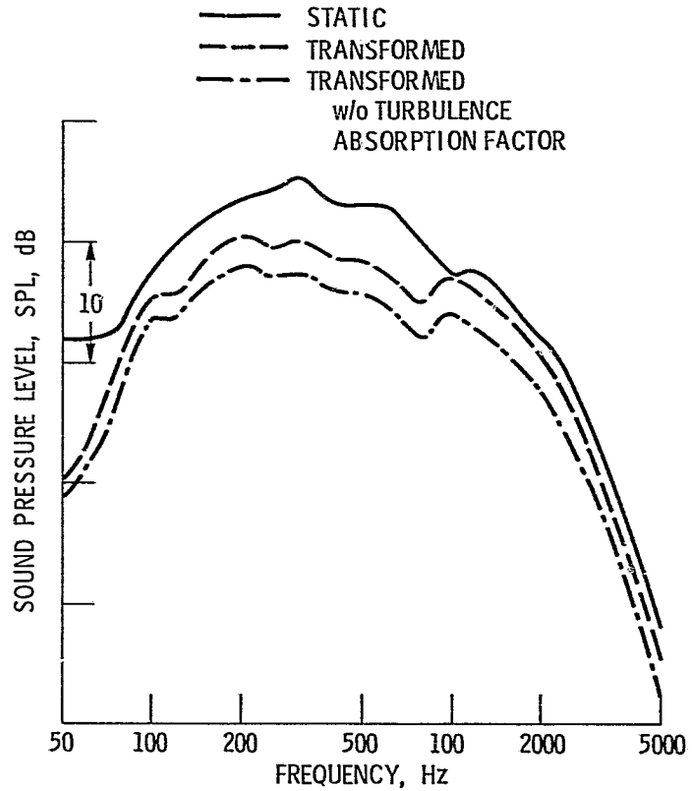

Figure 6. - Free jet spectra for conical nozzle from reference 10. V_j, 720 M/S; V_0, 122 M/S; nozzle area, 2181 cm^2; θ, 130^0; 732 m sideline distance.

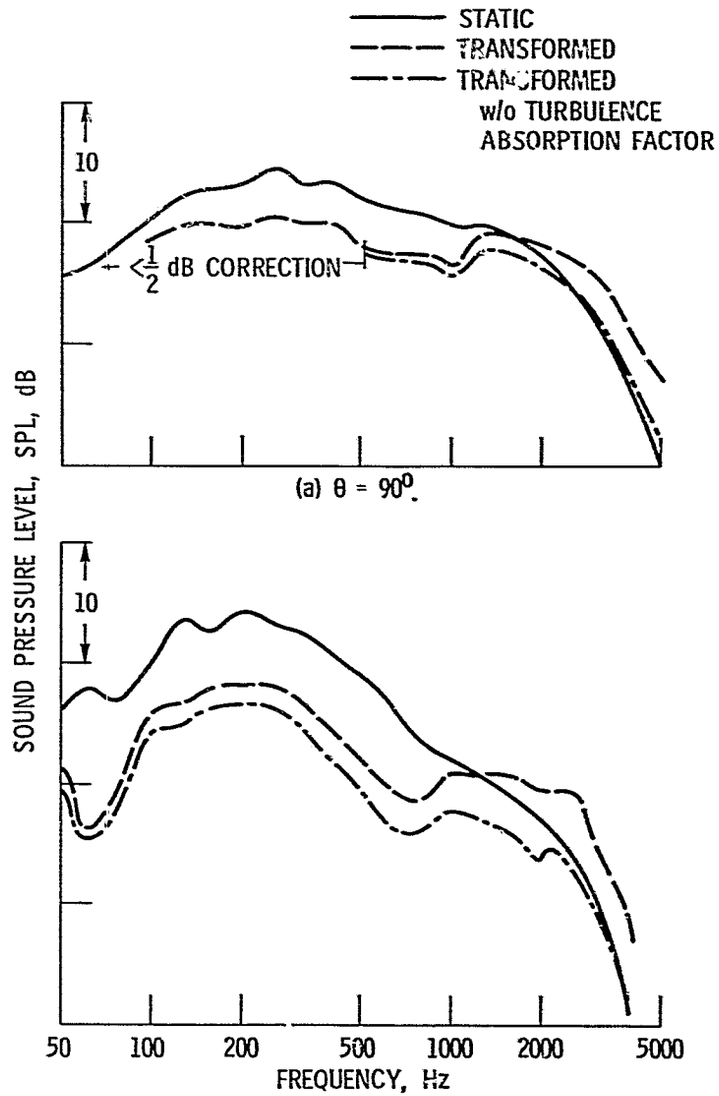

Figure 7. - Free jet spectra for 104-tube nozzle from reference 9. V_j, 732 M/S; V_0, 84 M/S; nozzle area, 2181 cm^2; 732 m sideline distance.

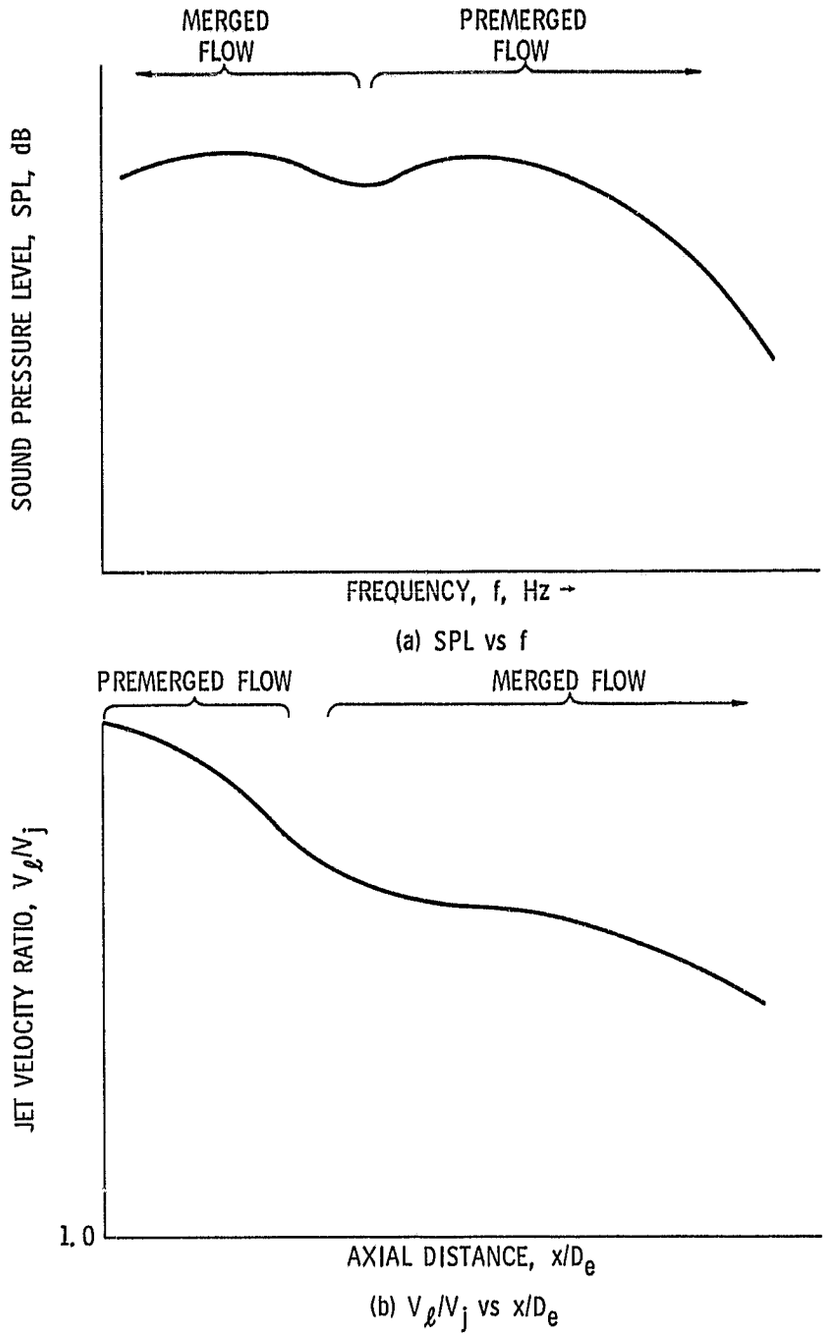

Figure 8. - Schematic sketch defining static SPL and jet velocity decay characteristics for a representative suppressor nozzle. Peak PNL angle.

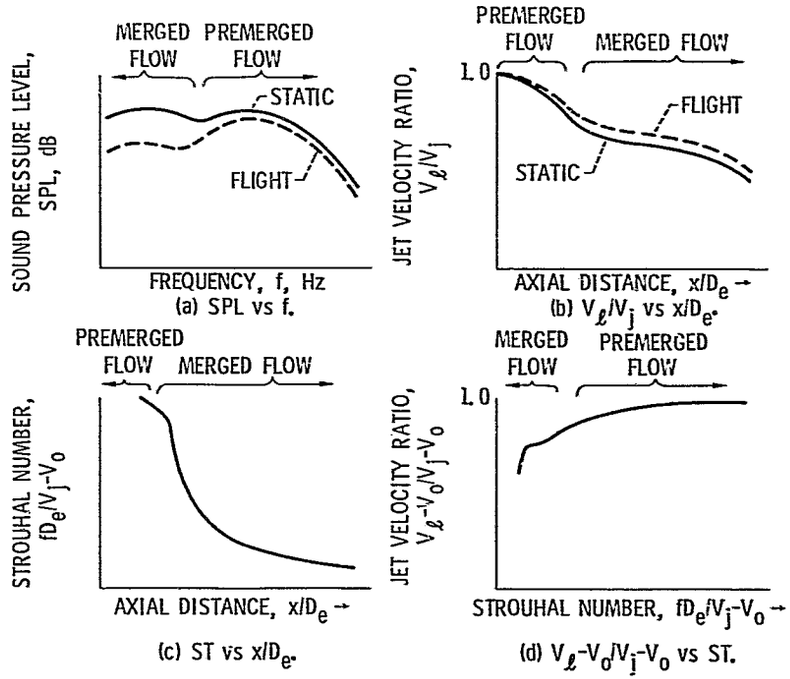

Figure 9. - Schematic sketch showing relationships of SPL, jet velocity ratio, and strouhal number for suppressor nozzle in-flight. Peak PNL angle.

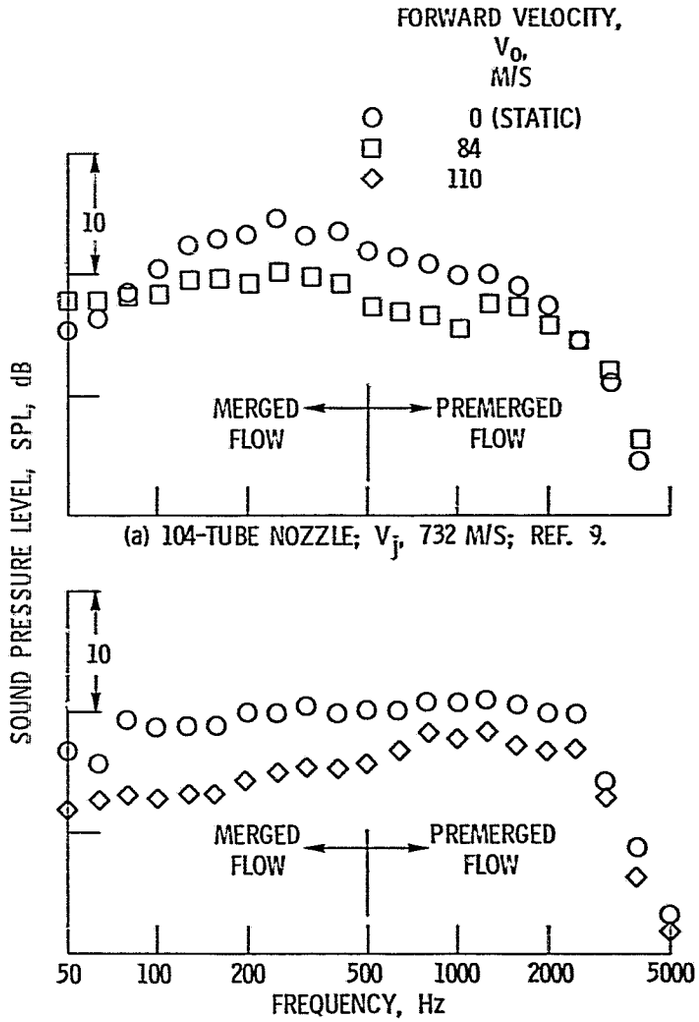

Figure 10. - Static and flight simulation spectra at $\theta = 90^0$ for several single-stream nozzles. Nozzle area, 2181 cm^2; 732 m sideline distance.

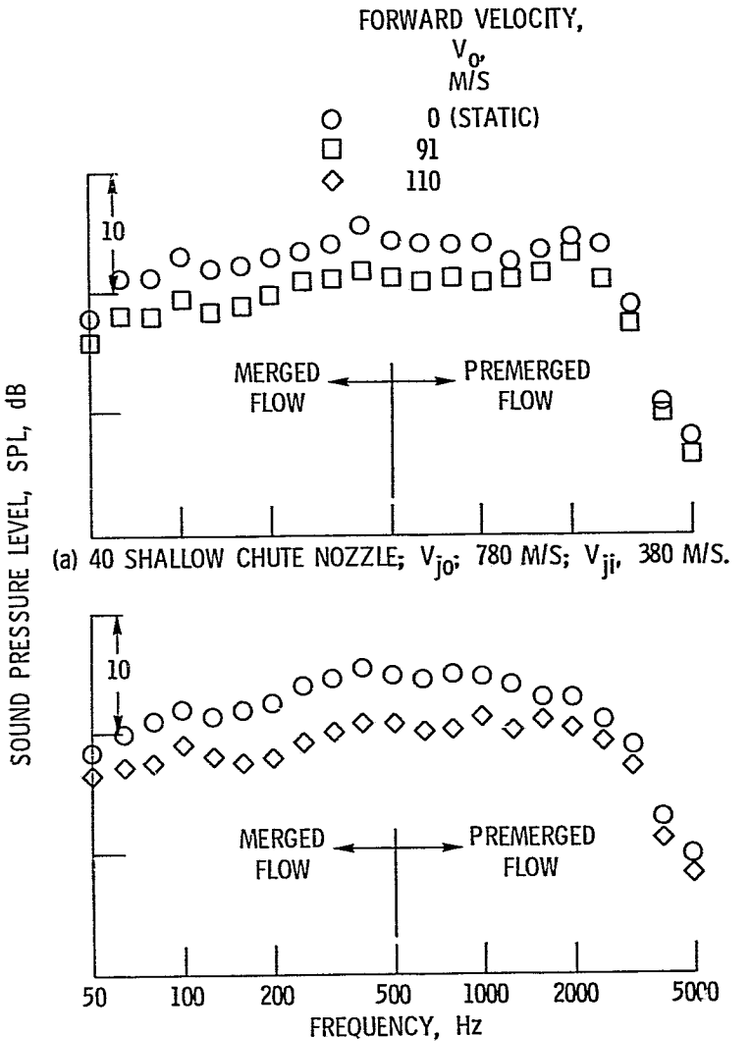

(a) 40 SHALLOW CHUTE NOZZLE; V_{j0}, 780 M/S; V_{ji}, 380 M/S.

(b) 36 CHUTE C-D NOZZLE; AR 2.0; V_{j0}, 780 M/S V_{ji}, 512, M/S.

Figure 11. - Static and flight simulation spectra at $\theta = 90^0$ for two coannular inverted-velocity-profile nozzles with outer stream suppressors. Total nozzle area, 2181 cm^2; 732 m sideline distance; ref. 10.

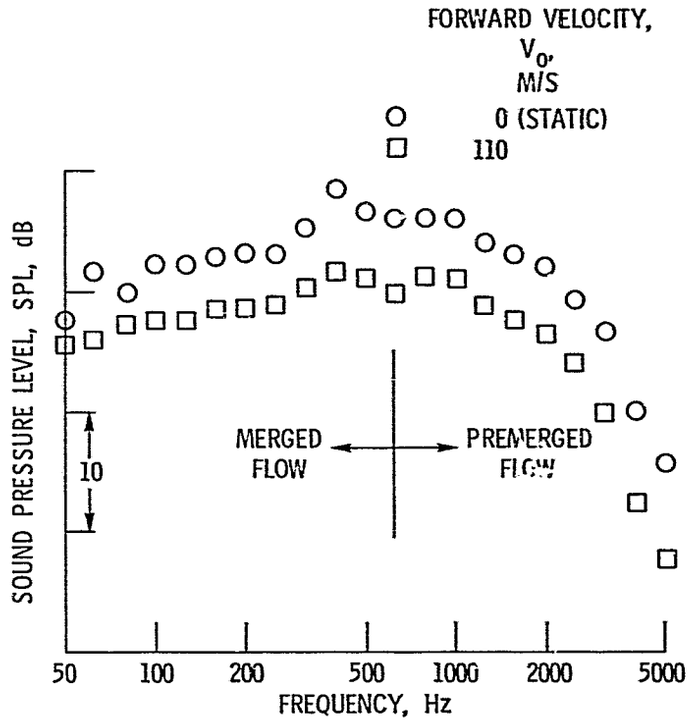

Figure 12. - Static and flight simulation spectra at $\theta = 90^0$ for a 54 element coplanar mixer nozzle. Nozzle area, 2181 cm^2; V_{j0}, 790 M/S; V_{ji}, 342 M/S; 732 m sideline distance; ref. 10.

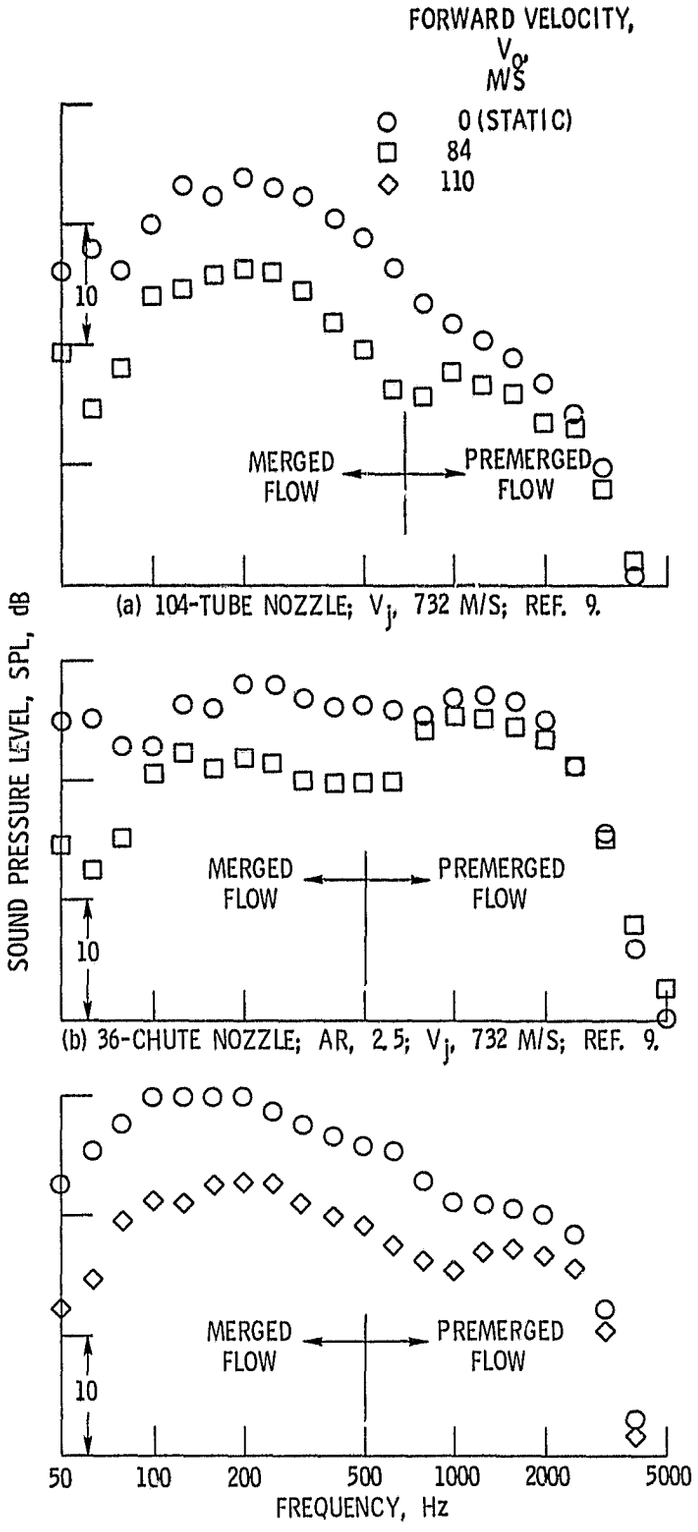

(a) 104-TUBE NOZZLE; V_j, 732 M/S; REF. 9.

(b) 36-CHUTE NOZZLE; AR, 2.5; V_j, 732 M/S; REF. 9.

(c) 32-CHUTE NOZZLE; AR, 2.1; V_j, 701 M/S; REF. 10.

Figure 13. - Static and flight simulation spectra at $\theta = 130^0$ for several single-stream nozzles. Nozzle area, 2181 cm^2; 732 m sideline distance.

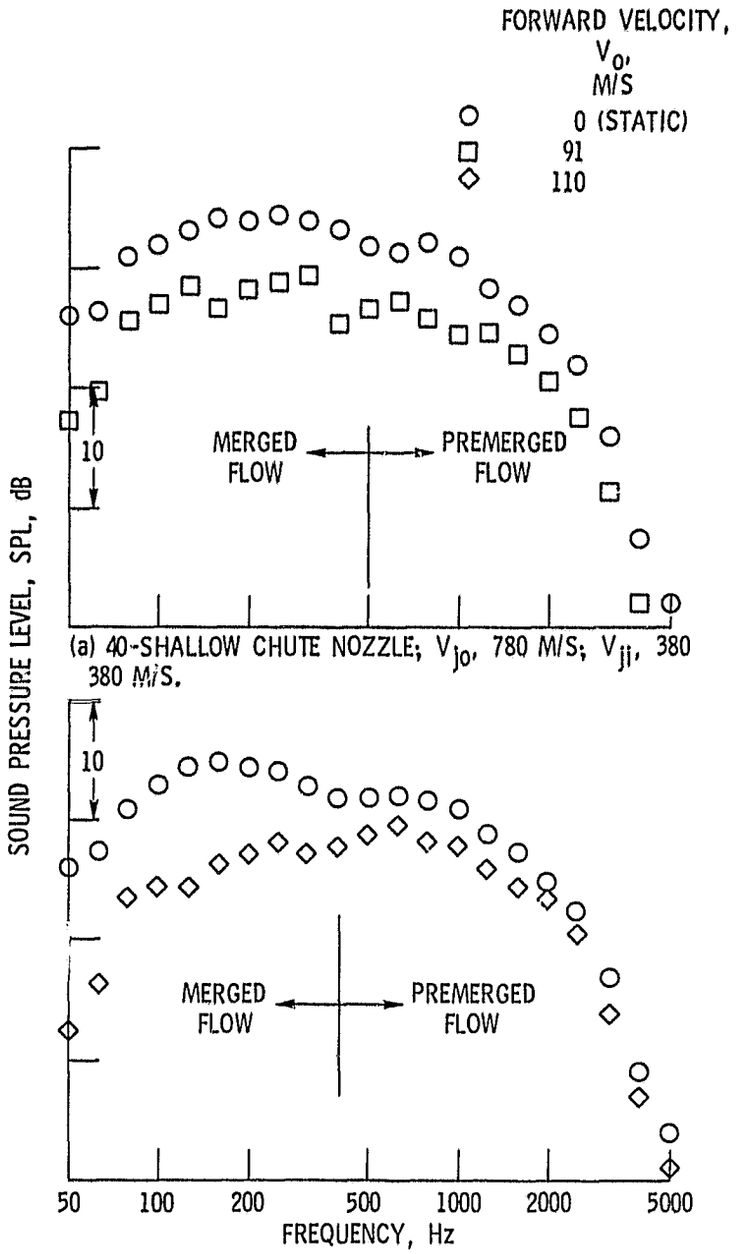

(a) 40-SHALLOW CHUTE NOZZLE; V_{jo}, 780 M/S; V_{ji}, 380 380 M/S.

(b) 36-CHUTE NOZZLE; AR, 2.0; V_{jo}, 780 M/S; V_{ji}, 512 M/S.

Figure 14. - Static and flight simulation spectra and $\theta = 130^0$ for two coannular inverted-velocity-profile nozzles with outer stream suppressors. Nozzle area, 2181 cm^2; 732 m sideline distance; ref. 10.

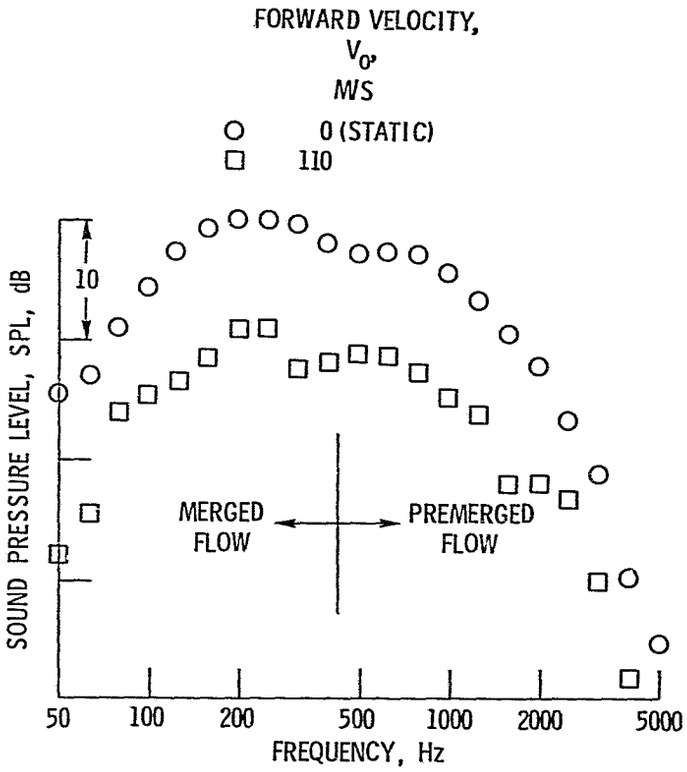

Figure 15. - Static and flight simulation spectra at $\theta = 130^0$ for a 54 element coplanar mixer nozzle. Nozzle area, 2181 cm^2; V_{jo}, 790 M/S; V_{ji}, 342 M/S; 732 m sideline distance; ref. 10.

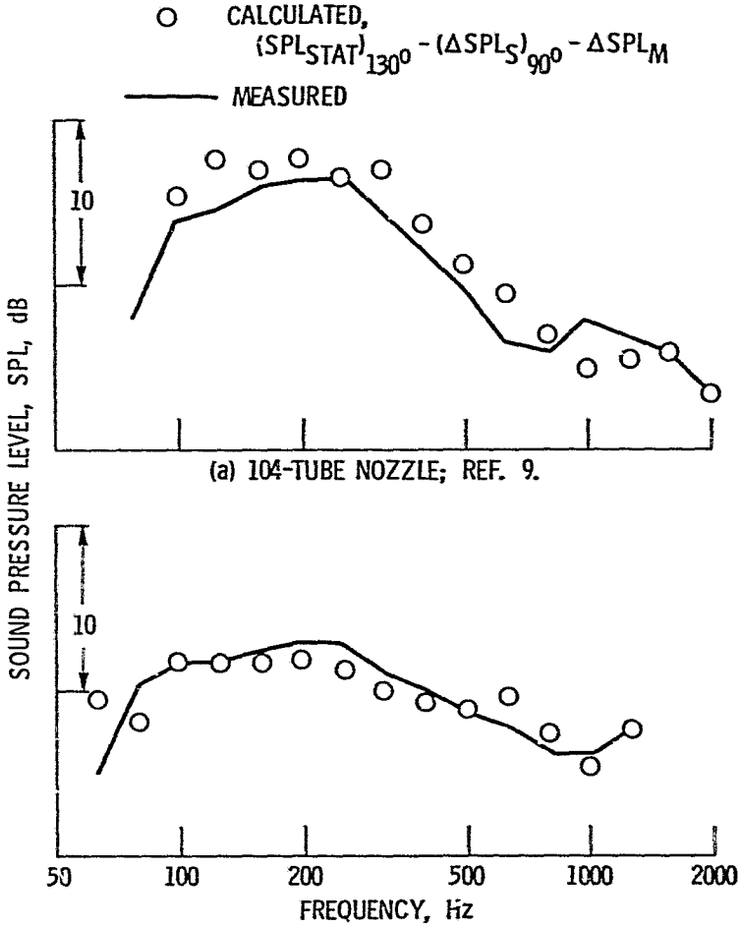

(a) 104-TUBE NOZZLE; REF. 9.

(b) 32-CHUTE NOZZLE; REF. 10.

Figure 16. - Comparison of measured inflight merged flow spectra at $\theta = 130^0$ with spectra calculated from sum of inflight data at $\theta = 90^0$ and moving medium effect. Single stream nozzles.

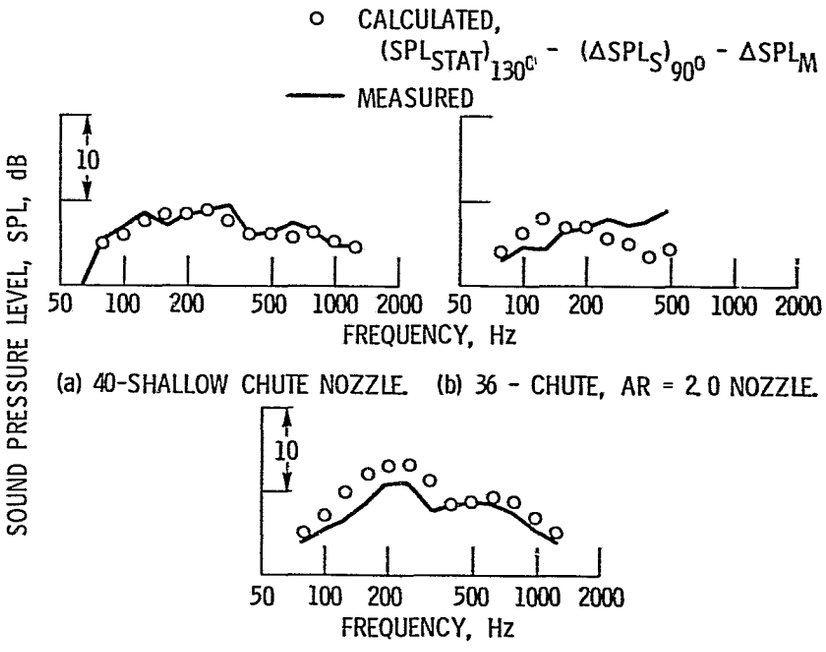

(a) 40-SHALLOW CHUTE NOZZLE. (b) 36 - CHUTE, AR = 2.0 NOZZLE.

(c) 54 ELEMENT COPLANAR MIXER NOZZLE.

Figure 17. - Comparison of measured inflight merged flow spectra at $\theta = 130^0$ with spectra from the sum of inflight data at $\theta = 90^0$ and moving medium effect. Dual stream nozzles. Ref. 10.

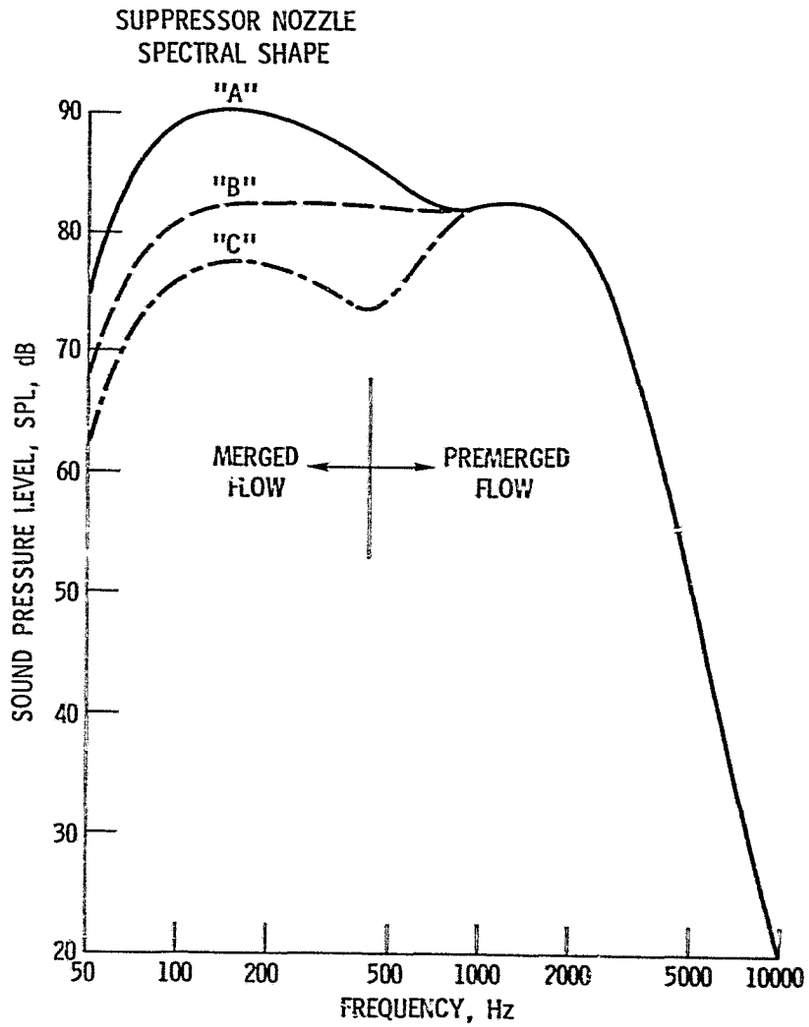

Figure 18. - Representative variations in suppressor nozzle spectral shapes at peak PNL angle. Jet velocity, 701 M/S; nominal nozzle area, 2181 cm^2; 732 m sideline distance.

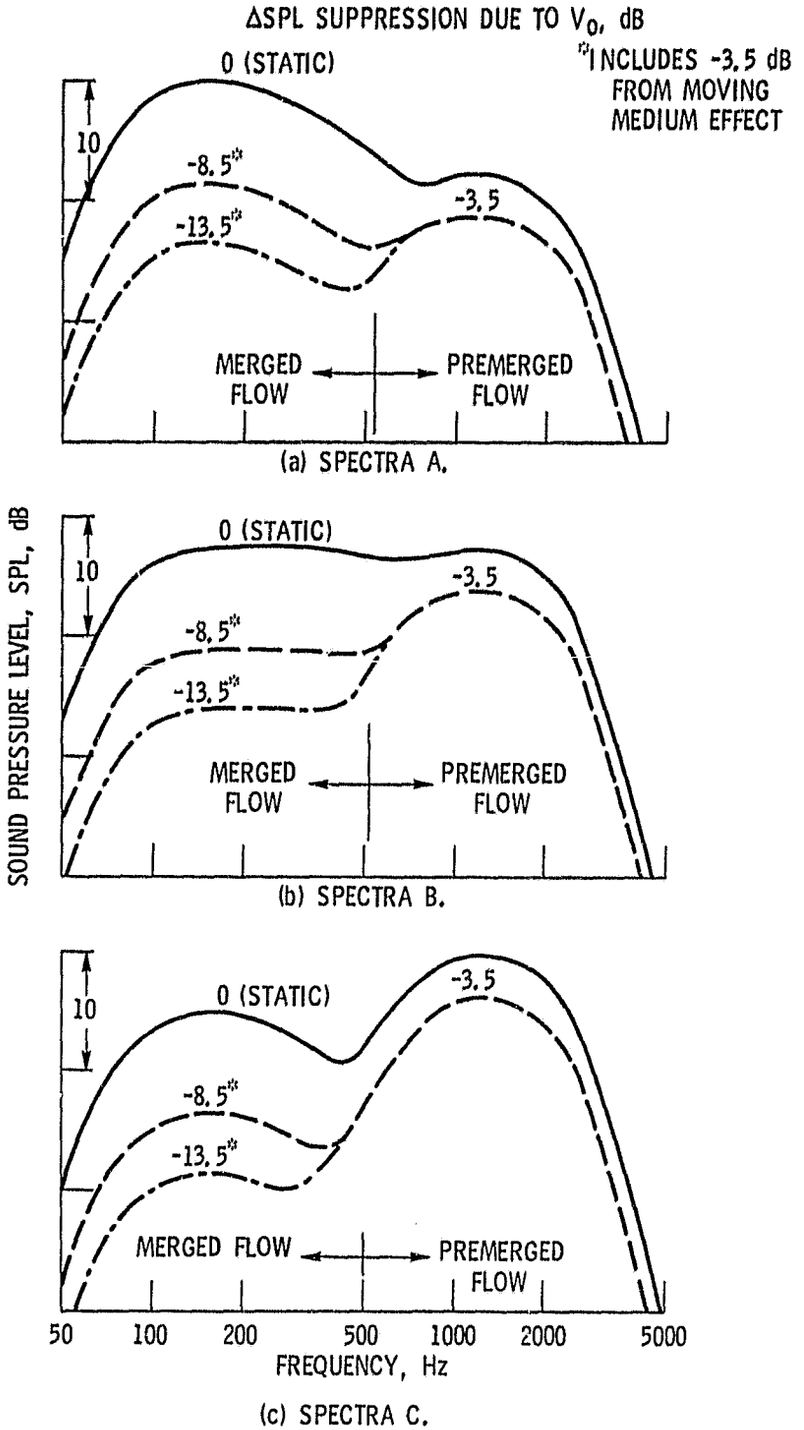

Figure 19. - Static and flight spectra for analysis of flight effects on suppressor nozzle noise at peak PNL angle ($\theta = 130^0$). V_j, 701 M/S; V_0 = 122 M/S; 732 m sideline.

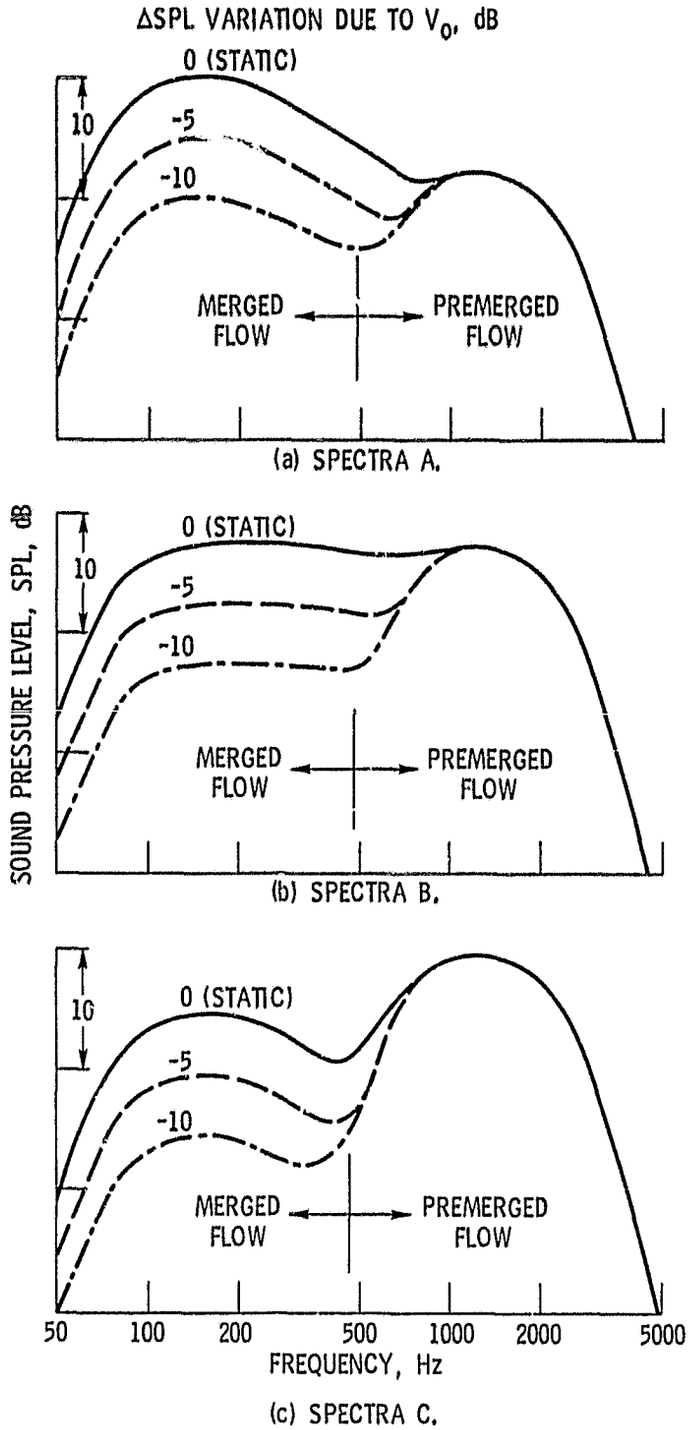

Figure 20. - Static and flight spectra for analysis of flight effects on suppressor nozzle noise at $\theta = 90^0$. V_j, 701 M/S; V_0, 122 M/S; 732 m sideline.

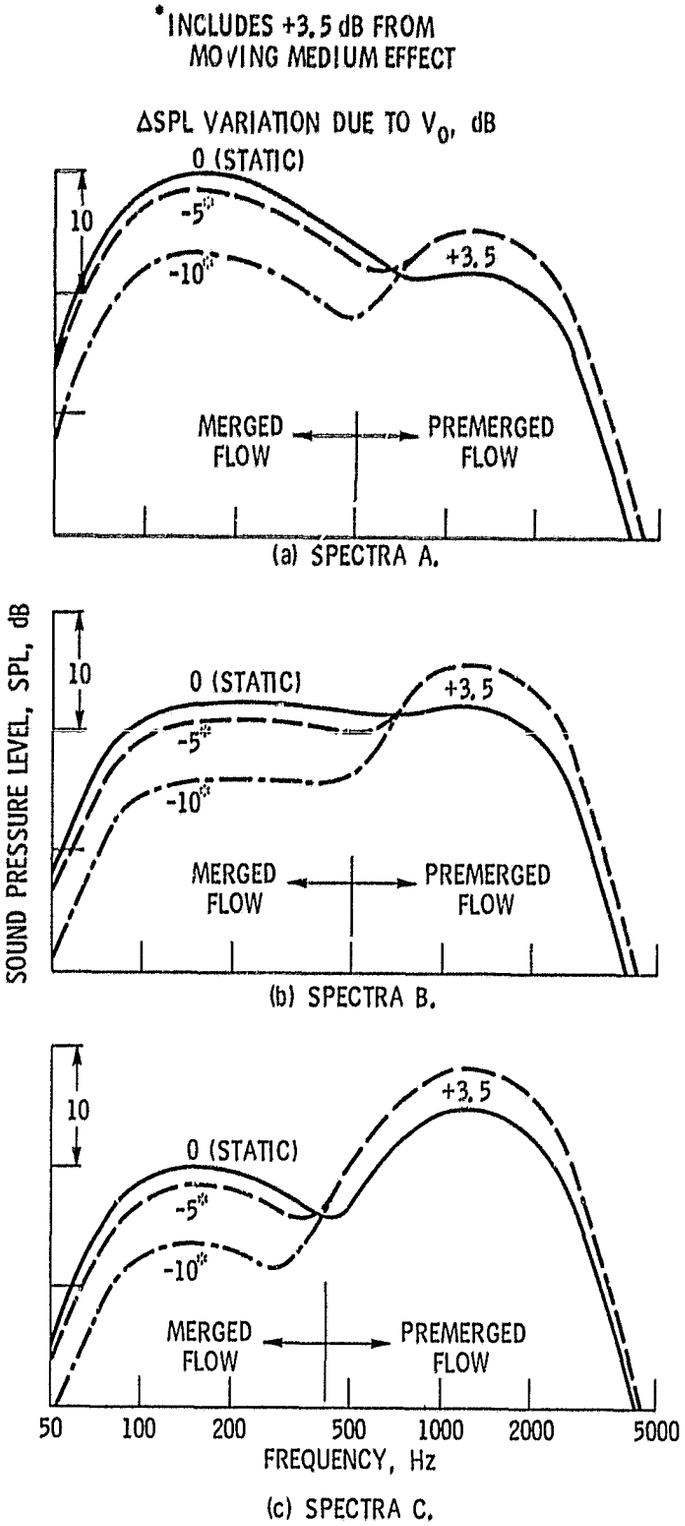

Figure 21. - Static and flight spectra for analysis of flight effects on suppressor nozzle noise in forward quadrant ($\theta = 50^0$). V_j, 701 M/S; V_0, 122 M/S; 732 m sideline.

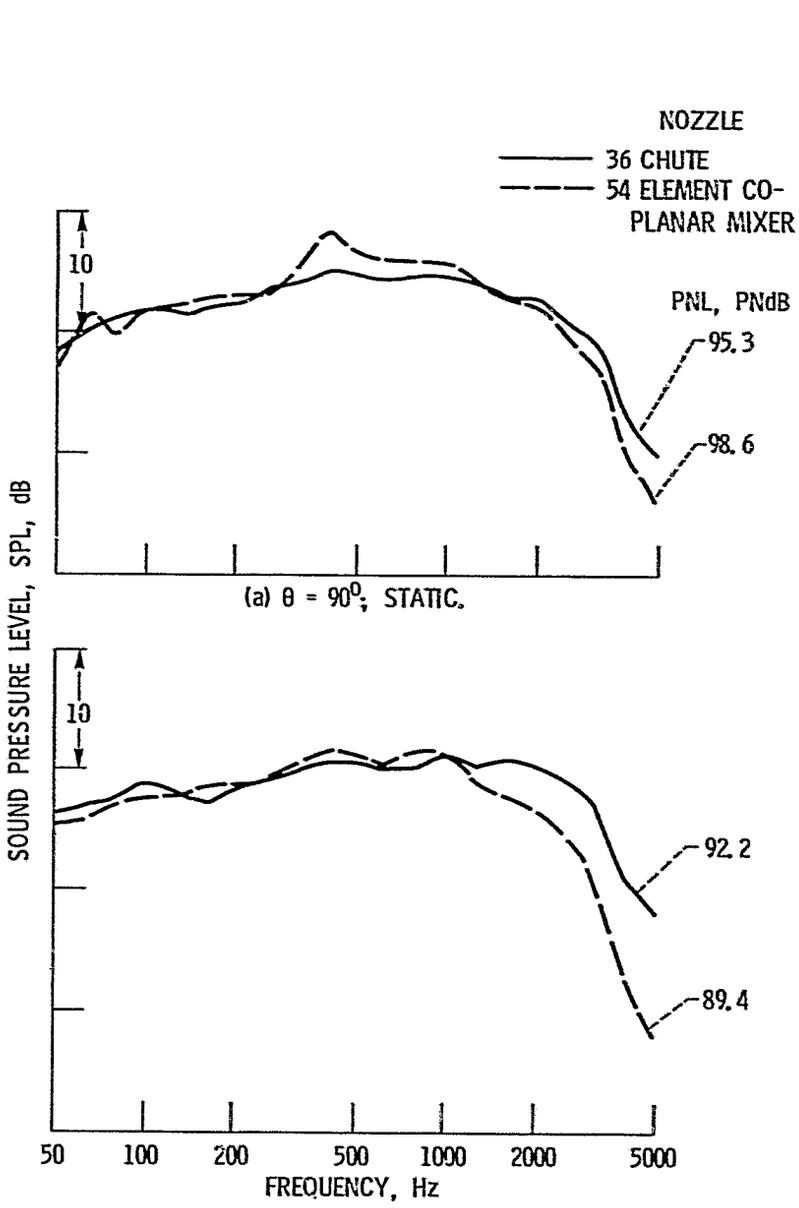

Figure 22. - Spectral comparisons between 54 element coplanar mixer nozzle and 36 chute suppressor nozzle. Ref. 10.

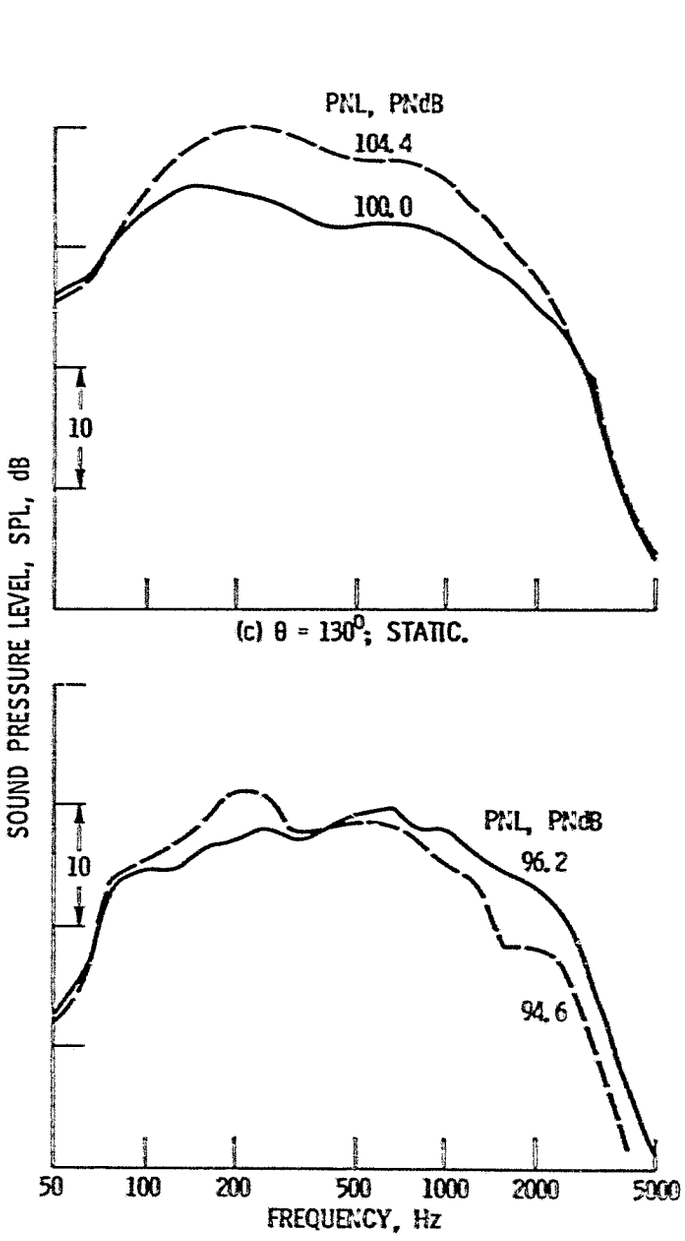

Figure 22. - Concluded.

1 Report No.	2 Government Accession No.	3 Recipient's Catalog No.
NASA TM-81377		

4 Title and Subtitle	5 Report Date
ACOUSTIC CONSIDERATIONS OF FLIGHT EFFECTS ON JET NOISE SUPPRESSOR NOZZLES	6 Performing Organization Code
7 Author(s) U. von Glahn	8 Performing Organization Report No. E-282
9 Performing Organization Name and Address National Aeronautics and Space Administration Lewis Research Center Cleveland, Ohio 44135	10 Work Unit No.
	11 Contract or Grant No.
12 Sponsoring Agency Name and Address National Aeronautics and Space Administration Washington, D.C. 20546	13 Type of Report and Period Covered Technical Memorandum
	14 Sponsoring Agency Code

15 Supplementary Notes

16 Abstract

Insight into the inflight acoustic characteristics of high-velocity jet noise suppressor nozzles for supersonic cruise aircraft (SCA) is provided. Although the suppression of jet noise over the entire range of directivity angles is of interest, the suppression of the peak noise level in the rear quadrant is frequently of the most interest. Consequently, the paper is directed primarily to the inflight effects at the peak noise level. Both single and inverted-velocity-profile multistream suppressor nozzles are considered. The importance of static spectral shape on the noise reduction due to inflight effects is stressed.

17. Key Words (Suggested by Author(s))	18. Distribution Statement
Jet noise	Unclassified - unlimited STAR Category 71

19. Security Classif. (of this report)	20. Security Classif. (of this page)	21. No. of Pages	22. Price*
Unclassified	Unclassified		

* For sale by the National Technical Information Service, Springfield, Virginia 22161